Electromagnetic and Thermal Properties of a Conductively Loaded Epoxy

E.J. Wollack[1], D.J. Fixsen[2], R. Henry[1], A. Kogut[1], M. Limon[2], P. Mirel[2]

Exploration of the Universe Divsion[1]
NASA Goddard Space Flight Center, Code 685
Greenbelt, MD 20771
email: edward.j.wollack@nasa.gov

Science Systems and Applications, Inc.[2]
NASA Goddard Space Flight Center, Code 685
Greenbelt, MD 20771

Keywords: Dielectric Mixtures, Microwave Absorbers and Terminations, Cryogenic Material Characterization

Abstract: We discuss the mechanical, thermal, and electromagnetic properties of a castable microwave absorber consisting of a mixture of stainless steel powder suspended in a commercially available epoxy. The resulting mixture is well suited for cryogenic applications. Its coefficient of thermal expansion closely matches most metals to reduce mechanical strain during cooldown. The absorption can be tuned by varying the volume filling fraction of the stainless steel powder in the mixture and exhibits little change from room temperature to 4 K. We provide simple expressions for the real and imaginary parts of the dielectric permittivity as a function of frequency and the stainless steel filling fraction.

Introduction: For many radiometric experiments it is convenient to have a highly absorptive (black) material with a good thermal conductance which can be easily thermally anchored to metals like copper or aluminum. Commercially available castable absorber formulations have a coefficient of thermal expansion which is poorly matched to these metals at cryogenic temperatures. This mismatch can result in the mechanical failure of the material and poses a limitation for their use at microwave wavelengths where the required coating thickness can be substantial. In this paper we discuss an epoxy loaded with stainless steel powder which has many useful properties as a cryogenic microwave absorber. In particular its coefficient of thermal expansion, 21-26 [10^{-6}/K], is well matched to commonly used metals and alloys. The stainless steel powder employed is a disordered system which introduces electromagnetic losses which only change slightly with temperature. The material can be cast at modest temperatures to form a variety of shapes and the stainless steel volume filling fraction can be varied to fine tune the absorption properties.

Here we report on the properties of a mixture made from a mechanically robust epoxy loaded with alumina, Emerson & Cuming 2850FT, and 5-30% stainless steel powder by volume. We refer to this class of absorbers made from readily available materials and appropriate for use at cryogenic temperatures as “Steelcast”. Experimental data on other commercially available castable absorber materials which have comparable electrical properties to the formulations studied here are described in [1-5]. The relatively poor coefficient of thermal expansion match of these formulations to metals can result in poor adhesion and unreliable mechanical performance due to the high internal stress upon cooling layer thicknesses greater than a centimeter. For these reasons, the mechanical properties of the composite described here are preferred for long wavelength cryogenic applications.

Thermal and Mechanical Properties: The thermal properties of Steelcast were measured by preparing three samples, each 9.5 mm diameter and 75 mm long with the procedure specified in Appendix A. The samples were 0%, 10%, and 30% steel powder by volume; but no significant differences in the thermal properties at low temperature were found. One end of each sample was fixed to a cold plate and a small heater was attached to the opposite end. Thermometers at 25 mm and 50 mm were used to record the temperature and the gradient for different temperatures of the cold plate from 5 to 25 K. The heater power required to drive a thermal gradient was then used to calculate the thermal conductivity of the material. The time required to come to equilibrium was used to estimate the heat capacity. An upper bound on the sample’s static electrical conductance was measured under vacuum. A hardness of 92 on the Shore D scale was observed for a 25% Steelcast sample (ASTM test method designation D2240 with a Shore Instruments Instron Durometer). These measurements and others of potential interest for the composite material are summarized in Table 1.

Electromagnetic Properties: A vast literature is devoted to the prediction and measurement of the constitutive parameters for such two-phase composite materials [6-11]. More recent reviews outlining the susceptibilities obtained with various theories and observed semi-empirical rules are can be found in [12,13]. In general, the electromagnetic response of a conductively loaded dielectric media is a function of the host dielectric constant, the inclusion particle geometry and conductivity, the volume filling fraction, and incident radiation wavelength.

The mixtures described here possess a separated-grain structure whose dielectric properties can be approximated by the Maxwell-Garnet effective media theory up to ~0.5 THz. This approximation assumes that the inclusions are spherical, randomly dispersed throughout the host medium, and exhibit macroscopic uniformity on the scale of the radiation wavelength. In this limit, the dielectric function of the composite dielectric, ε_{eff}, is related to that of the host, ε_h, and inclusion, ε_i, media by

$$\frac{\varepsilon_{eff} - \varepsilon_h}{\varepsilon_{eff} + 2\varepsilon_h} = f \cdot \frac{\varepsilon_i - \varepsilon_h}{\varepsilon_i + 2\varepsilon_h}$$

where f is the volume filling fraction of the inclusion medium [14]. For metallic inclusions ε_i is large and imaginary, resulting in a lossy dielectric mixture with tunable properties. Deviations from this simple relationship are anticipated for large filling fractions. These effects can be accounted for following the formulation of Neelakanta [15,16] through the introduction of effective depolarization factors.

The size distribution of the 16 micron mesh stainless steel powder used in this investigation is presented in Figure 1. The observed uniformity of this material's composition and size is sufficient to have negligible variability on the modeled electromagnetic performance of the composite mixture at millimeter wavelengths. In the infrared, extinction from the mixture was observed to be consistent with the anticipated limitations of the simple theory used to model the response. Formation of a percolation conduction matrix at zero frequency does not occur in these formulations for several reasons: The native refractory oxides which reside on the surface of the stainless steel are essentially insulating, the few micron sized alumina particles used in the 2850 FT to achieve high thermal conductivity are electrically insulating and further limit conductive pathways through the material, and stainless steel volume fractions above ~0.3 are difficult to achieve in practice with these mixtures.

A Fabry-Perot resonator technique was used to derive the material's optical constants from the observed electromagnetic response. We outline the data analysis approach used for the test samples depicted in Figure 2. In extracting the constitutive relations for the samples, we assume a complex permittivity and permeability for the sample which varies smoothly with frequency:

$$\varepsilon \equiv \varepsilon_r^* \varepsilon_o = \left(\varepsilon_r' + i\varepsilon_r''\right) \cdot \varepsilon_o$$
$$\mu \equiv \mu_r^* \mu_o = \left(\mu_r' + i\mu_r''\right) \cdot \mu_o$$

where $\varepsilon_o \approx 8.854 \times 10^{-12}$ F/m and $\mu_o = 4\pi \times 10^{-7}$ H/m respectively and express the propagation constant in the unfilled and mixture filled waveguide regions as

$$\gamma_o = -i\sqrt{\left(\frac{\omega}{c}\right)^2 - \left(\frac{2\pi}{\lambda_c}\right)^2}$$
$$\gamma = -i\sqrt{\left(\frac{\omega}{c}\right)^2 \mu_r^* \varepsilon_r^* - \left(\frac{2\pi}{\lambda_c}\right)^2}$$

where ω is the angular frequency of the incident radiation and c is the speed of light in the vacuum. The geometry defining the waveguide which holds and illuminates the sample determines the cutoff wavelength, λ_c, for the structure [17]. The scattering parameters for the resonator formed by the contrast between the filled and unfilled sections guiding the light can be expressed as follows,

$$S_{11} = S_{22} = \left[\frac{\left(1 - z^2\right)\Gamma}{1 - z^2\Gamma^2}\right]$$
$$S_{21} = S_{12} = \left[\frac{\left(1 - \Gamma^2\right)z}{1 - z^2\Gamma^2}\right]$$

which are the complex field reflection and transmission coefficients for the structure under test. For convenience we define, $\Gamma \equiv \left(\gamma_o/\mu_o - \gamma/\mu\right)/\left(\gamma_o/\mu_o + \gamma/\mu\right)$ and $z \equiv \exp(-\gamma L)$, where L is the sample thickness and the reference planes are at the front and back interfaces of the sample.

In choosing the sample thickness for the measurements we note that electrically thin (thick) samples with low (high) loss provide information about the real (imaginary) component of the propagation constant. To achieve the desired accuracy for the real and imaginary components of the constitutive parameters two shim thickness are employed: The first is chosen to result in 1 to 3 Fabry-Perot resonances over the 30% fraction waveguide band and the second is several e-folding lengths. In extracting the constitutive relations from the rectangular waveguide data we enforce causality following the method of Baker-Jarvis et al. [18]. We destructively test the witness coupons to verify that voids and other defects are not present. In principle, the single-mode approximation implicitly employed in the above analysis may be violated by the excitation of higher order modes if the test sample is not homogeneous. This condition can systematically increase the measured loss over the simple single mode theoretical approximation.

We measure the material properties as a function of stainless steel volume filling fraction by using a set of specially fabricated Fabry-Perot resonator samples. An HP 8510C vector network analyzer is used to measure the each sample's scattering parameters a function of frequency. Typical test data is presented in Figures 3a and 3b. In Figure 4, the measured complex relative permittivity is summarized for rectangular waveguide (WR28.0) samples at 30 GHz. Similarly, this approach is used to characterize the frequency dependence of a set of Steelcast samples with 30% stainless steel loading by volume. See Figure 5. For these tests, samples in assorted standard rectangular waveguides (i.e., WR284, WR187, WR112, WR90.0, WR28.0, and WR10.0) were fabricated and characterized.

The submillimeter properties for 0, 10, and 25% Steelcast volume filling fractions were characterized at 5 and 300 K with a Bruker IFS 113V Fourier transform spectrometer (FTS). To model the observed FTS spectra, we evaluate the expressions given above in the infinite cutoff wavelength limit, $\lambda_c \to \infty$ and use the measured sample thickness. See Figure 6 for a summary of these measurements. For the FTS beam divergence, spot size and sample geometry, the structure is effectively a one-dimensional Fabry-Perot resonator (i.e., plane wave illumination of a single dielectric layer bounded by vacuum). The derived dielectric parameters from these measurements are also included in Figure 5.

The observed dielectric properties for the steel loaded epoxy samples were essentially constant from ~4 to 300 K. These observations are consistent with expectations given the small changes in sample geometry and the composite material's constituent component properties with temperature. The key to producing this response is that the dominant component of the loss in the material mixture is the steel powder, a disordered alloy, whose conductivity does not appreciably change over the temperate range of interest. This property enables one to use room temperature measurements of components utilizing these formulations to provide useful guidance of the cryogenic performance. Although a permanent magnet attracts the stainless steel powder, the observed relative magnetic permeability for all the formulations studied is consistent with unity in the wavebands characterized.

It is commonly necessary to specify the required coating thickness for the material to achieve the desired level of attenuation. We recall, for a homogenous half space of a lossy dielectric, the complex refractive index of the material, $\hat{n} = n + i\kappa$,

$$n = \sqrt{\frac{1}{2} \cdot \left(\sqrt{\varepsilon_r'^2 + \varepsilon_r''^2} + \varepsilon_r' \right)}$$

$$\kappa = \sqrt{\frac{1}{2} \cdot \left(\sqrt{\varepsilon_r'^2 + \varepsilon_r''^2} - \varepsilon_r' \right)}$$

can be expressed [20] in terms of the relative dielectric permittivity, $\varepsilon_r^* = \varepsilon_r' + i \cdot \varepsilon_r''$, which have been experimentally determined. To facilitate numerical estimates we provide the approximate dielectric fitting functions summarizing the measured data in Figures 4 and 5. For volume filling fractions, $0 < f < 0.3$, the 30 GHz observations are qualitatively reproduced by the fitting functions $\varepsilon_r'(30\,GHz, f) \approx 5.2 \cdot e^{2.5f}$ and $\varepsilon_r''(30\,GHz, f) \approx 0.1 + 1.9f + 22.4f^2$. For frequencies between, $3 < \nu < 300$ GHz, the samples with 30% volume filling fraction the data are qualitatively reproduced by the fitting functions $\varepsilon_r'(\nu, 0.3) \approx 13.8 \cdot \nu^{-0.07}$ and $\varepsilon_r''(\nu, 0.3) \approx 3.4 \cdot \nu^{-0.07}$. The inverse of the extinction length, the attenuation constant, α, for a homogenous lossy dielectric layer is,

$$\alpha = \frac{2\pi}{\lambda_o} \cdot \kappa = \frac{2\pi}{\lambda_o} \cdot \sqrt{\frac{\varepsilon_r'}{2} \cdot \left(\sqrt{1 + \tan^2 \delta} - 1 \right)},$$

where λ_o is the free space wavelength of the incident radiation. In the limit the loss tangent, $\tan\delta = \varepsilon_r''/\varepsilon_r'$, becomes large, the required thickness to produce significant attenuation falls; however, the corresponding Fresnel reflection losses for an unmatched layer becomes appreciable. These considerations are crucial in use of these materials for applications where high emmisivity or reflection reduction with minimal volume is required.

Conclusion: At microwave through infrared wavelengths, conductively loaded dielectric materials are used in a variety of technological applications ranging from electromagnetic absorbing coatings to passive thermal control. We summarize the measured mechanical and electrical properties of a versatile composite material suitable for use at cryogenic temperatures. The observed coefficient of thermal expansion is appropriately matched for repeated thermal cycling when bonded to aluminum, copper, or steel structures. Through the use of a disordered metal alloy, stainless steel powder, as the loading inclusions in the host media; the resulting material properties are essentially temperature independent and controllable by varying the volume fraction. The resulting formulations are highly repeatable and well suited for cryogenic radiometric applications.

APPENDIX A: Steelcast Sample Preparation Procedure

The following components are used in the preparation of the Stycast – stainless steel powder mixtures we refer to as Steelcast:

Emerson & Cuming Stycast 2850 FT, Catalyst 23 LV [21]
Carpenter 16 micron Stainless Steel Powder Micro-Melt 316L [22]

The vendor specifies a density for Stycast 2850 FT in the range of ~2.35 to 2.45 g/cm^3. This variability in density can have a significant influence on the complex dielectric constant and was traced to settling of the Al_2O_3 in the 2850 FT over the timescale of weeks. We alleviate this issue by mixing the 2850 FT in the storage container for about 2-3 minutes prior to transferring the required amount of material to a separate mixing container. Next, the 2850 FT is heated in a mixing container to 40 to 50 C for about 30 minutes. Catalyst 23 LV (7.5% by weight) is added and mixed vigorously for ~3 minutes. Stainless steel powder (30% by volume, 59% by weight) is then added and mixed vigorously for ~3 minutes or until the mixture is smooth and free of clumps. Acetone (up to 12% by volume) can be added to make the mixture easier to pour and cast, however, this increases the curing time by up to 300% if used in a mold with limited openings for venting. The introduction of acetone reduces the elasticity and mechanical strength of the resulting material as indicated in Table 1. Other material properties of the final product are largely unaffected by the addition of acetone during the casting process.

The mixture is then degassed in order to remove the air incorporated during mixing by placing in a vacuum-oven at a ~40 to 50 C and evacuating to <6.5 kPa. The mixture will rapidly rise when the pressure drops to ~15 kPa and then collapse. After the mixture collapses, it is degassed for about 30 seconds and then returned to ambient pressure. At this point the material is removed from vacuum and gently folded without re-incorporation of air. Since the material quickly thickens upon cooling, for best results, it is poured into the intended mold as soon as practical. The addition of carbon black to these mixtures is recommended if a lower DC conductivity is required.

The properties of the Steelcast formulations described can be well controlled: Over the course of a year, 36 individual waveguide shim samples (WR28.0) were filled with the 30% Steelcast formulation and a complex dielectric constant of $\varepsilon_r^* = 10.8 + 2.4i$ ($\mu_r^* \approx 1$) with a 4% scatter in the derived parameters. The highest dielectric volume loading fraction explored in practice was realized by an alternative method – a mold was filled with stainless steel powder and cyanoacrylate (i.e., "superglue") was employed as the host dielectric media. To eliminate the formation of voids in the sample; after packing, the binder was pulled through the steel powder with a vacuum pump. The observed electrical properties at 30 GHz for this composite material were $\varepsilon_r^* \sim 20 + 20i$ and $\mu_r^* \approx 1$.

REFERENCES:

[1] Eccosorb Lossy, Magnetically Loaded Castable Resin (CR) Machinable Stock (MF) Absorbers, Emerson & Cuming Microwave Products, Randolph, MA 02368; (http://www.eccosorb.com).

[2] J.B. Peterson and P.L. Richards, "A Cryogenic Blackbody for Millimeter Wavelengths," 1984, Int. J. Infrared & Millimeter Waves, Vol. 5, No. 12, pp. 1507-1515.

[3] H. Hemmati, J.C. Mather, and W.L. Eichhorn, "Submillimeter and Millimeter wave Characterization of Absorbing Materials," 1985, Applied Optics, Vol. 24, No. 24, pp. 4489-4492.

[4] M. Halpern, H.P. Gush; E. Wishnow; V. de Cosmo, "Far Infrared Transmission of Dielectrics at Cryogenic and Room Temperatures - Glass, Fluorogold, Eccosorb, Stycast, and Various Plastics," 1986, Applied Optics, Vol. 25, No. 2, pp. 565-570.

[5] A.R. Kerr., H. Moseley, E.J. Wollack, W. Grammer, G. Reiland, R. Henry, K.P. Stewart, "MF-112 and MF-116: Compact Waveguide Loads and FTS Measurements at Room Temperature and 5 K," 2004, ALMA Memo 494; (http://www.alma.nrao.edu/memos/); G.A. Ediss, A.R. Kerr, H. Moseley, K.P. Stewart, "FTS Measurements of Eccosorb MF112 at Room Temperature and 5 K from 300 GHz to 2.4 THz," 1999, ALMA Memo 273; (http://www.alma.nrao.edu/memos/).

[6] J. W. Rayleigh, “On the Influence of Obstacles Arranged in Rectangular Order Upon the Properties of a Medium,” 1892, Philosophical Magazine, Vol. 34, pp. 481-502.

[7] J.C. Maxwell Garnett, “Colours in Metal Glasses and in Metallic Films,” 1904, Philosophical Transactions of Royal Society of London, A, Vol. 203, pp. 385-420; J.C. Maxwell Garnett, “Colours in Metal Glasses, in Metallic Films, and in Metallic Solutions. II,” 1906, Philosophical Transactions of Royal Society of London, A, Vol. 205, pp. 237-288.

[8] K. Lichtenecker, “Calculation of Resistance of Alloys Free from Solid Solutions,” 1909, Phys. Zeitschr., Vol. 10, pp. 1005-1008.

[9] D.A.G. Bruggemann, “The Calculation of Various Physical Constants of Heterogeneous Substances, 1. The Dielectric Constants and Conductivities of Mixtures Composed of Isotropic Substances,” 1935, Annalen Der Physik, Vol. 24, pp. 636-664 (in German).

[10] H. Fricke, “A Mathematical Treatment of the Electrical Conductivity and Capacity of Disperse Systems I,” 1924, Physical Review, Vol. 24, pp. 575-587; H. Fricke, “A Mathematical Treatment of the Electrical Conductivity and Capacity of Disperse Systems II,” 1926, Physical Review, Vol. 26, pp. 678-681.

[11] L. Lewin, “The Electrical Constants of a Material Loaded with Spherical Particles,” 1947, Institution of Electrical Engineers (London) Journal, Part 3, Radio and Communication Engineering, Vol. 94, pp. 65-68.

[12] S.A. Paipetis, G.M. Tsangaris, J. M. Tsangaris, “Dielectric Properties of Metal-Filled Epoxies,” 1983, Polymer Communications, Vol. 24, pp. 373—375.

[13] D.S. McLachlan, A. Priou, I. Chenerie, and E. Issac, “Modeling the Permittivity of Composite Materials with a General Effective Medium Equation,” 1992, Journal of Electromagnetic Waves and Applications, Vol. 6, No. 9, pp. 1099-1131.

[14] G.A. Niklasson, C.G. Granqvist, O. Hunderi, “Effective Medium Models for the Optical Properties of Inhomogeneous Materials,” 1981, Applied Optics, Vol. 20, No. 1, pp. 26-30.

[15] P.S. Neelakanta, “Permittivity of Dielectric-Conductor Mixture: Application of Logarithmic Law of Mixing to Electric Susceptibility,” 1989, Electronics Letters, Vol. 25, No. 12, pp. 800-802 and references therein.

[16] S. Kisdnasamy and P.S. Neelakanta, “Complex Permittivity of a Dielectric Mixture: Modified Fricke’s formula Based on Logarithmic Law of Mixing,” 1984, Electronics Letters, pp. 291-292.

[17] N. Marcuvitz, *Waveguide Handbook,* 1951, MIT Radiation Laboratory Series, McGraw-Hill, New York, Vol. 10.

[18] J. Baker-Jarvis, R.G. Geyer, P.D. Domich, “A Nonlinear Least-Squares Solution with Causality Constraints Applied to Transmission Line Permittivity and Permeability Determination,” 1992, IEEE Transactions on Instrumentation and Measurement, Vol. 41, No. 5, pp. 646-652.

[19] A. Donev, I. Cisse, D. Sachs, E.A. Variano, F.H. Stillinger, R. Connelly, S. Torquato, P.M. Chaikin “Improving the Density of Jammed Disordered Packings Using Ellipsoids,” 2004, Science, Vol. 303, No. 2, pp. 990-993

[20] A. Von Hippel, *Dielectrics and Waves,* 1954, Wiley, New York, pp. 26-28.

[21] Emerson & Cuming, "Stycast 2850 FT Thermally Conductive Epoxy Encapsulant," Technical Data Sheet, 1755-2850-FT/06-01; "Stycast 2850 FT Two Component, Versatile Epoxy Encapsulant with High Thermal Conductivity," Technical Data Sheet, E290/09/99-RVH/MVR.

[22] Micro-Melt 316L, 16 micron mesh stainless steel powder; Carpenter Powder Products Inc., 600 Mayer Street, Bridgeville, PA 75017.

Table 1: Selected Steelcast Material Properties

Parameter	Magnitude	Units	Notes
Appearance			Dark Gray in Color
Density, Constituents			
Al_2O_3	4.0 +/-0.2	[g/cm^3]	
Stainless Steel Powder	8.1+/-0.2	[g/cm^3]	
Stycast 2850 FT Epoxy	2.2+/-0.2	[g/cm^3]	
Density, by formulation			Catalyst: #23 LV
Steelcast (10% by Volume)	2.8 +/- 0.1	[g/cm^3]	
Steelcast (25% by Volume)	3.7 +/- 0.1	[g/cm^3]	
Steelcast (30% by Volume)	3.9 +/- 0.1	[g/cm^3]	
Thermal Expansion	21	[10^{-6}/K]	77 – 295 K
	26	[10^{-6}/K]	12% Acetone Dilution
Heat Capacity	740	[J/kg/K]	300 K
	$0.55\,T^2$	[J/kg/K]	Cryogenic (4 – 20 K)
Thermal Conductivity	$75\,T$	[nW/m/K]	Cryogenic (4 – 20 K)
Electrical Resistivity	$>8.4\times10^8$	[ohm-cm]	
Shore D Hardness	92	[-]	Undiluted Formulation
Elasticity	8.5 +/- 0.5	[GPa]	Undiluted Formulation
	0.3 +/- 0.05	[GPa]	12% Acetone Dilution
Mechanical Strength	85 +/- 5	[MPa]	Undiluted Formulation
	9 +/- 1	[MPa]	12% Acetone Dilution

Stycast 2850 FT Catalyst		**#9**	**#23 LV**	**#11**	Ref. [21]
Dielectric Function @ 1 MHz:		5.01	5.36	5.36	[-]
Dissipation Factor @ 1 MHz:		0.028	0.051	0.043	[-]
Volume Resistivity @ 25C		$>10^{+15}$	$>10^{+15}$	$>10^{+15}$	[ohm-cm]
Dielectric Strength		14.4	14.8	15	[V/μm]
Outgassing, TML		0.25		0.29	[%]
Thermal Conductivity		1.25	1.02	1.28	[W/m-K]
Glass Transition Temperature,	T_g	86	68	115	[C]
Thermal Expansion Coefficient:	$T < T_g$	35	39.4	31.2	[10^{-6}/K]
	$T > T_g$	98.9	111.5	97.9	[10^{-6}/K]

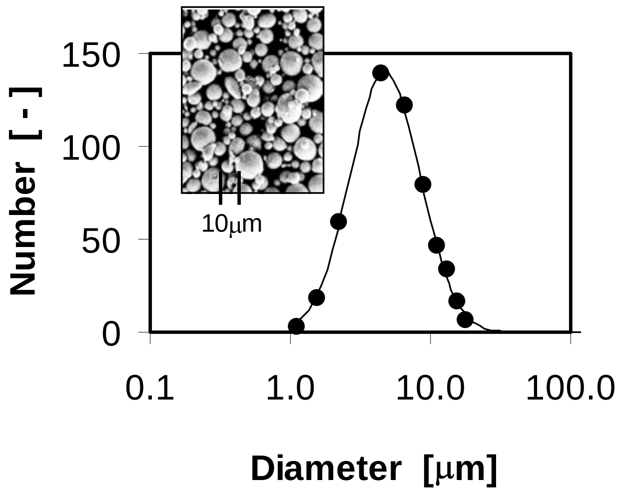

Figure 1: Stainless Steel Powder Particle Size Distribution. The 16 micron mesh stainless steel particles employed are approximately spherical in shape and follow a log-normal distribution (diameter: mode 4.8 microns, average 8.3 microns; sample size: 522 particles). The insert is a scanning electron microscope image of a representative sample of the material.

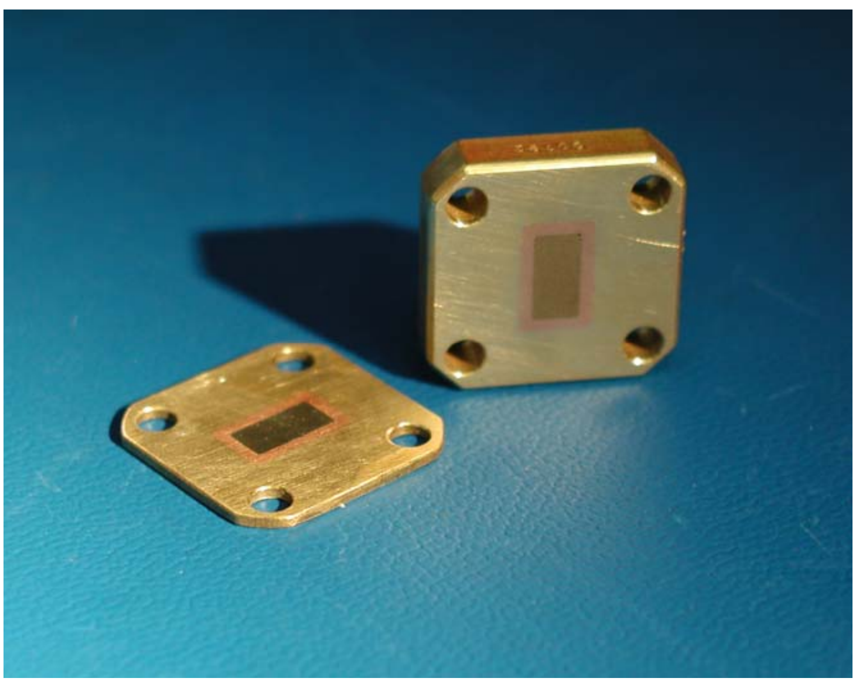

Figure 2: Waveguide Resonator. Standard WR28.0 waveguide flanges with copper waveguide are potted with Steelcast and lapped to the desired thickness.

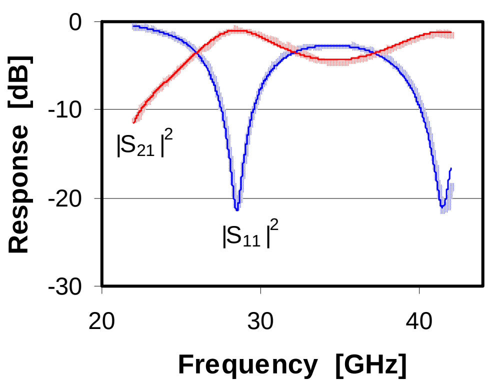

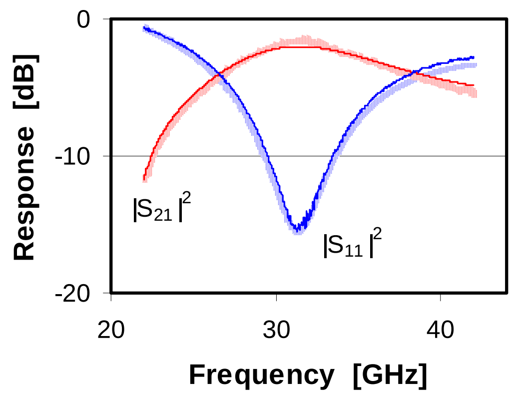

Figure 3a and 3b: Measured and Modeled Waveguide Resonator Response. In figure "3a", the scattering parameters for a WR28.0 (guide broadwall width 0.280" (7.11 mm); height 0.140" (3.56 mm)) waveguide sample, 0.192" (4.87 mm) long, filled with 2850 FT Stycast are indicted. Shaded and solid lines denote the transmission line model and measured data; red and blue coloration denote the sample reflection, $|S_{11}|^2$, and transmission, $|S_{21}|^2$, respectively. The plot linewidths indicated are representative of the systematic errors in the measurements with the HP8510C vector network analyzer. We note that the dielectric parameters extracted by fitting to observed spectra are in agreement with previous measurements [4], $\varepsilon_r^* = 5.22 + 0.10i$ and $\mu_r^* \approx 1$. In Figure "3b", a waveguide sample, 0.0762" (1.94 mm) long, is filled with Stycast loaded with 10% stainless steel by volume. For this mixture formulation, $\varepsilon_r^* = 6.55 + 0.55i$ and $\mu_r^* \approx 1$, was derived from the measured data.

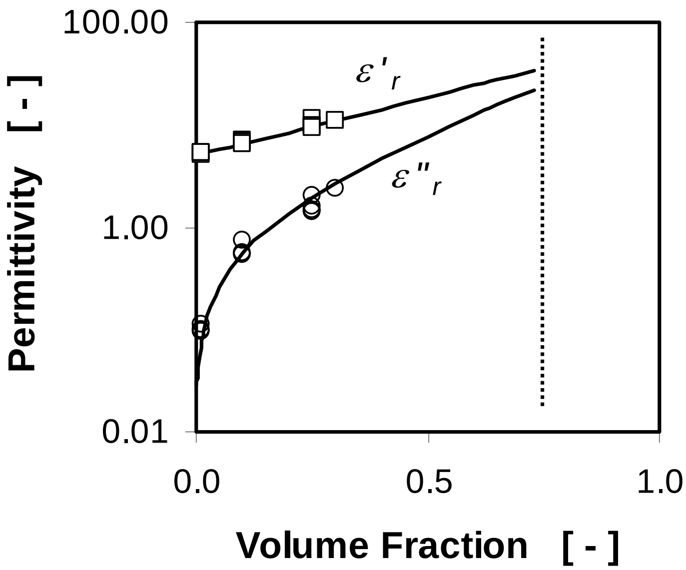

Figure 4: Steelcast Relative Permittivity as a Function of Volume Filling Fraction (Frequency = 30 GHz). The squares and circles indicate the measured real and imaginary components of the relative dielectric function respectively. For the model we evaluate the dielectric response at 30 GHz under the assumption that the metallic particles are ~8 micron in diameter. Volume filling fractions up to 0.3 are achievable with a 2850FT dielectric host by dilution with acetone to improve the mixing and casting properties. The vertical dotted line indicates the maximum fraction set by the inclusion geometry and size distribution [19].

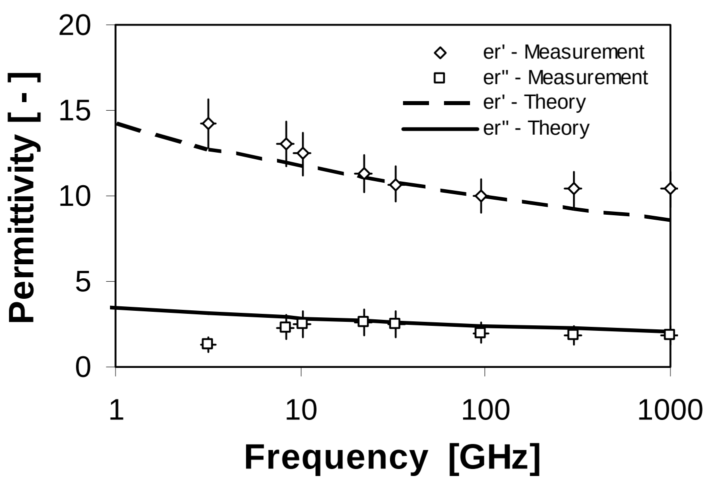

Figure 5: Steelcast Relative Permittivity as a Function of Frequency (Stainless Steel Volume Loading Fraction = 30%). The squares and circles indicate the measured real and imaginary components of the relative dielectric function respectively. The lines indicate the corresponding modeled parameters.

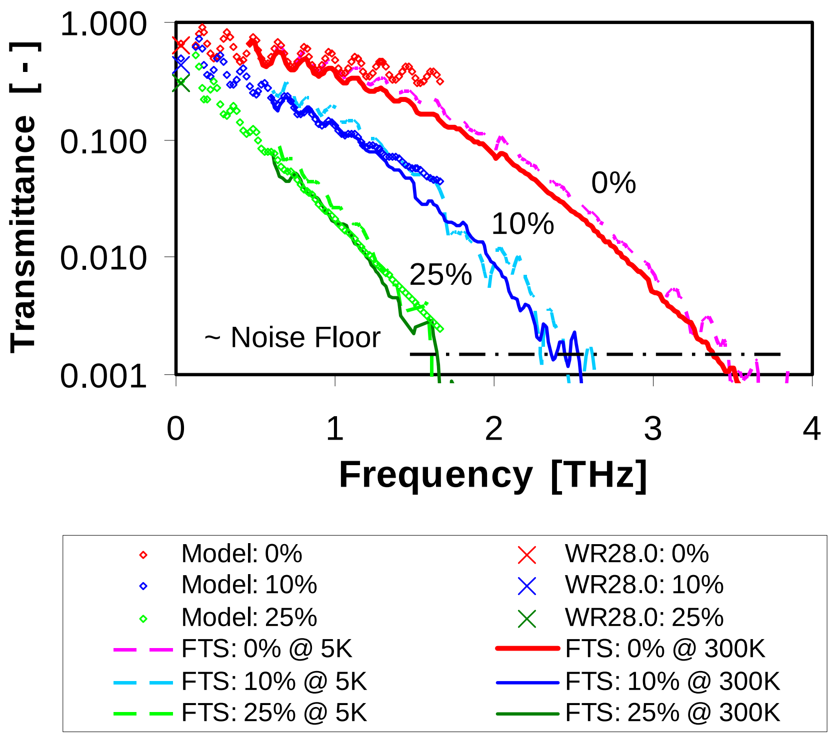

Figure 6: Steelcast Sample Fourier Transform Spectrometer Response. The spectra were measured at physical temperatures of 5 and 300 K with a Bruker IFS 113V Fourier transform spectrometer. Transmittance data is presented for Steelcast samples lapped to a thickness of 40 microns with volume filling fractions of 0, 10, and 25%. Reflectance data taken on the 0% sample indicates that the extinction due to diffuse scattering from the alumina particles is significant above ~1.5 THz. The diamonds are the modeled response for the sample; the crosses are the corresponding measurements of the waveguide samples acquired with the vector network analyzer.